WEP Warwick Evans Publishing

Academic Journal of Management Science and Engineering

ISSN: 3080-9827 (Print), ISSN: 3080-9835 (Online) | Volume 1, Number 2, Year 2026
DOI: https://doi.org/10.62051/ajmse.v1n2.19
Journal homepage: https://ajomse.com



Experimental Study on the Mechanical Response and Seepage Characteristics of Low-Permeability Reservoirs under Pressure-Driven Water Injection Conditions

Mengqi Wang

College of Petroleum Engineering, Xi'an Shiyou University, Xi'an, Shaanxi, 710000, China

ABSTRACT

To address the issues of insufficient injection capacity and slow energy replenishment associated with conventional waterflooding development in low-permeability oil reservoirs, this study takes typical low-permeability core samples from the X block in the eastern Yin'e Basin as the research subject. A systematic series of experiments on rock mechanics, single-phase and two-phase seepage, and imbibition is carried out to reveal the mechanical response of the reservoir, the evolution of seepage capacity, and the redistribution characteristics of residual oil under pressure-driven water injection conditions. The results indicate that pressure-driven water injection can significantly improve pore-throat connectivity and flow pathways, thereby enhancing the co-permeability of oil and water phases. In addition, imbibition oil displacement facilitates further mobilization of residual oil in medium and large pores.

KEYWORDS

Low-permeability Reservoir; Pressure-driven Water Injection; Rock Mechanics; Imbibition.

1. INTRODUCTION

Conventional waterflooding development in low-permeability oil reservoirs generally faces challenges such as insufficient injection capacity, slow formation energy replenishment, and difficulty in effectively establishing an injection–production pressure differential[1] .Pressure-driven water injection, which achieves rapid pressurization and synergistic displacement through high-pressure, high-rate injection, has emerged as a key technology for improving the development performance of such reservoirs. To experimentally elucidate the permeability-enhancing and oil-displacement mechanisms of pressure-driven water injection, this study takes typical low-permeability core samples from the X block as the research subject. A series of diverse experiments are systematically conducted to clarify the intrinsic mechanisms by which pressure-driven water injection improves the seepage conditions of low-permeability reservoirs and enhances oil displacement efficiency, from two perspectives: fracture-induced permeability enhancement and alteration of oil–water migration regimes.

2. GEOLOGICAL CHARACTERISTICS OF THE BLOCK

The Chagan Depression is located in the central part of the Chagandelesu Depression in the eastern Yin'e Basin, within the territory of Inner Mongolia[2].The X block is structurally situated in the southern part of the Wuliji fault nose structural belt of the Chagan Depression, representing a consequent fault-nose structure developed on the downthrown side of the Maoxi Fault, with an area of 230 km². The Bayingebi Formation serves as the primary target interval, characterized by fan-delta

Content from this work may be used under the terms of CC BY-NC 4.0 licence (https://creativecommons.org/licenses/by-nc/4.0/).
Published by Warwick Evans Publishing.

deposits with small sedimentary body dimensions and rapid facies changes. The physical properties of the reservoir are generally tight.

3. EXPERIMENTAL SAMPLES AND METHODS

3.1. Experimental Samples

Table 1. Parameters of experimental samples

Sample No.	Porosity (%)	Permeability (mD)	Well depth (m)	Sample length (cm)	Sample diameter (cm)
1	3.856	2.015	2660.1	5.210	2.450
2	2.273	1.21	2662.7	5.295	2.448
3	2.421	1.67	2661.3	5.216	2.295

3.2. Experimental Procedure

(1)**Rock mechanics experiment**: To investigate the characteristics of rock deformation and failure as well as the mechanical conditions for fracture initiation under high-pressure conditions[3]. A triaxial rock mechanics system was used, with the load incrementally applied until core failure occurred. The compressive strength, Young's modulus, Poisson's ratio, and stress–strain relationship were obtained.

(2)**Single-phase seepage experiment**: To elucidate the regulatory effects of displacement pressure differential and injection rate on core seepage capacity. A core flooding system was employed, and formation water was displaced at pressure differentials ranging from 2 to 50 MPa and injection rates from 0.01 to 1 mL/min. Changes in permeability and porosity under different conditions were measured.

(3)**Oil–water two-phase seepage experiment**: To determine the influence of displacement pressure on oil–water two-phase flow and oil displacement efficiency. Using the same core, oil–water displacement tests were conducted at pressure differentials of 2, 4, and 8 MPa. Relative permeability curves were measured, and the variations in the co-permeability interval and residual oil saturation were analyzed.

(4)**Imbibition experiment**: Cores No. 2 and No. 3 were selected for static spontaneous imbibition experiments over 72 hours. Prior to the experiment, the cores were saturated with crude oil, placed in a sealed container, completely immersed in simulated formation water, and left to stand under constant temperature conditions. The imbibition oil production was recorded at regular intervals, the variation of imbibition volume over time was analyzed, and the spontaneous imbibition oil displacement capacity of different cores was evaluated.

4. RESULTS AND ANALYSIS

4.1. Rock Mechanics Experiment

Using a triaxial rock mechanics testing system, loading tests were conducted on Core No. 1 under a confining pressure of 23 MPa to obtain parameters such as compressive strength, Young's modulus, and Poisson's ratio[4]. Based on the effective stress theorem, the weakening effect of increased pore

pressure on rock strength was analyzed. The elastic constants of the core sample were determined from the linear segment of the stress–strain curve, which in this experiment was taken as the section between 45% and 70% of the maximum axial stress difference. The mechanical properties of the core sample are presented in the table below(table.2).

Table 2. Results of rock mechanics experiment

Effective confining pressure (MPa)	Compressive strength (MPa)	Young's modulus (MPa)	Shear modulus (MPa)	Bulk modulus (MPa)	Poisson's ratio
23.0	370	5.85E+04	2.27E+04	4.55E+04	0.2

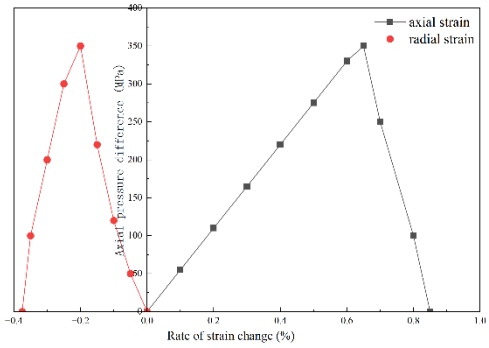


Figure 1. The stress-strain curve

In this experiment, conducted under an effective confining pressure of 23.0 MPa, the measured compressive strength of the core was 370 MPa, with a Young's modulus of 5.85×10^4 MPa, a shear modulus of 2.27×10^4 MPa, a bulk modulus of 4.55×10^4 MPa, and a Poisson's ratio of 0.286. The stress-strain curve (Figure 1) indicates that: the core loading process exhibits typical brittle failure characteristics: the axial stress difference increases approximately linearly with strain, reaching peak strength at a strain of about 0.65%, after which the stress drops rapidly, showing pronounced brittle instability. The radial strain exhibits little change during the initial loading stage but increases significantly as the peak strength is approached, reflecting the initiation and propagation of microcracks within the core and a notable volumetric dilation effect. The high Young's modulus, high compressive strength, and moderate Poisson's ratio indicate that the core possesses high stiffness and strong brittleness, making it prone to brittle fracturing under high stress, thereby providing favorable mechanical conditions for fracture initiation and propagation during pressure-driven water injection. Furthermore, although the reservoir rock exhibits a relatively high compressive load-bearing capacity, high-pressure water injection reduces the effective stress and elevates the pore pressure, thereby weakening the rock strength and further promoting fracture development. These findings provide a mechanical basis for the field application of pressure-driven water injection.

4.2. Single-Phase Flow Experiment

Through two sets of single-phase flow experiments with gradients of displacement pressure differential and injection rate, the evolution laws of core permeability and porosity under pressure-driven conditions were revealed[5]. The results are as follows:

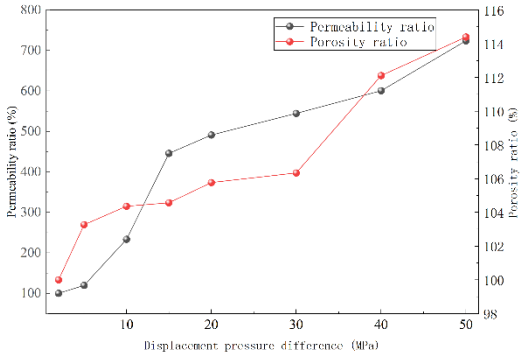


Figure 2. Displacement pressure differential

(1) Displacement pressure differential

As shown in Figure 2, with the displacement pressure differential gradually increasing from 2 MPa to 50 MPa, the core permeability ratio exhibits a significant nonlinear increase, rising from 100% to approximately 725%. In contrast, the porosity ratio increases only slightly, from 100% to about 115%. The marked difference in the magnitude of increase between the two parameters indicates that the enhancement of permeability by high-pressure displacement is far greater than that of porosity. The underlying mechanism is not simply the expansion of pore volume, but rather the opening and connection of numerous originally closed microcracks and isolated pore throats within the core through the wedging and scouring action of high-pressure fluid, thereby forming a seepage channel network with high flow conductivity.

When the pressure differential is below 10 MPa, the increase in permeability is limited. When the pressure differential exceeds 10 MPa, the slope of the permeability curve increases significantly, indicating that the reservoir enters a "rapid permeability-enhancement stage dominated by fracture opening." At 50 MPa, the permeability increase exceeds six times the initial value, confirming that high-pressure perturbation is a key factor in improving the seepage capacity of low-permeability reservoirs.

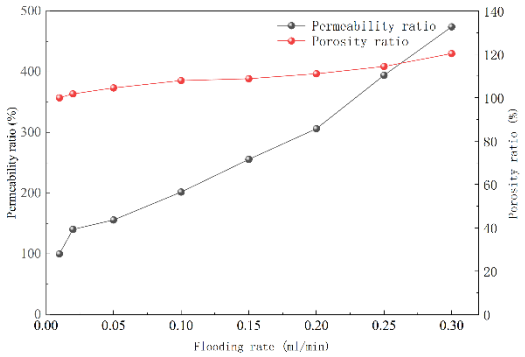


Figure 3. Injection rate

(2) Injection rate

As shown in Figure 3, with the injection rate increasing from 0.01 mL/min to 0.3 mL/min, the core permeability ratio also exhibits a significant increasing trend, rising from 100% to approximately 475%. In contrast, the porosity ratio increases only slowly from about 100% to approximately 120%, with the magnitude of increase again being much smaller than that of permeability.

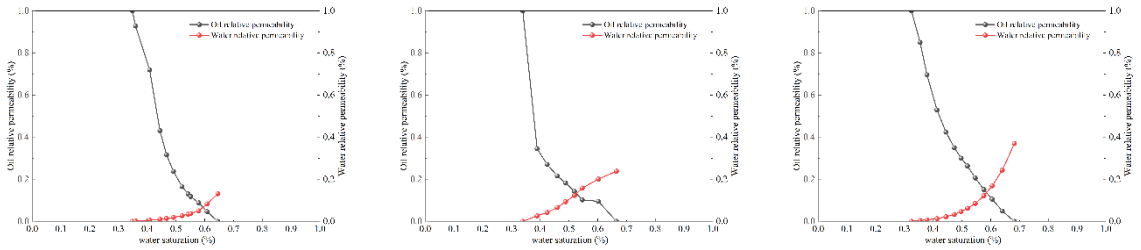
In the low-rate stage (0.01-0.05 mL/min), the increase in permeability is relatively small, mainly reflecting the migration of impurities within the pores and minor adjustments of pore throats. In the medium-to-high-rate stage (0.05-0.3 mL/min), the permeability increase accelerates markedly, indicating that a higher injection rate can enhance the scouring effect on fracture surfaces through

shear stress, further widening and connecting the already opened fracture channels, thereby improving the overall flow conductivity.

Synthesizing the results from both sets of experiments, it can be concluded that the displacement pressure differential is the primary driving force for improving the seepage capacity of low-permeability reservoirs, achieving a stepwise increase in permeability by reducing effective stress and opening microcracks. The injection rate serves as an auxiliary factor, optimizing the flow conductivity of seepage channels through fluid shear action. The synergistic effect of the two jointly establishes a "pore–fracture composite seepage system," providing an experimental basis for the efficient application of pressure-driven water injection technology in low-permeability oil reservoirs.

4.3. Two-Phase Flow Experiment

Using the same core sample, oil–water relative permeability tests were conducted at displacement pressures of 2, 4, and 8 MPa, and parameters such as irreducible water saturation, residual oil saturation, and the co-permeability interval were obtained[6]. The characteristics of the oil–water relative permeability curves under different displacement pressure conditions are shown in Figure 4. The variations in the curves reflect the regulatory effect of the pressure of pressure-driven water injection on the two-phase flow behavior of oil and water in low-permeability reservoirs.



a.2MPa b.4MPa c.8MPa

Figure 4. The characteristics of the oil–water relative permeability curves under different displacement pressure conditions

As the displacement pressure increases from 2 MPa to 8 MPa, the oil–water relative permeability curves exhibit regular variations: the oil-phase curve shifts upward as a whole with a slower decline, while the water-phase curve also shifts upward with a faster rise. The co-permeability interval of the oil and water phases expands significantly, and the iso-permeability point moves toward the lower water saturation direction. Under low-pressure conditions, the flow capacity of the oil phase declines rapidly with a high residual oil saturation, and the water phase is difficult to mobilize with large flow resistance. As the pressure increases, the mobilized range of the oil phase expands, the residual oil saturation decreases, and the water phase more readily forms continuous flow channels, resulting in a marked enhancement of its flow capacity.

Increasing the displacement pressure can weaken the flow interference between the oil and water phases, improve the fluid flow conditions within the pore–fracture composite channels, expand the two-phase co-permeability interval, reduce the residual oil saturation, and enhance the water-phase flow capacity, thereby effectively increasing the sweep volume of waterflooding and the degree of crude oil mobilization.

4.4. Imbibition Experiment

To clarify the spontaneous imbibition oil displacement characteristics of different cores, a 72-hour static imbibition experiment was conducted[7]. The variation of imbibition volume over time for the

two core samples (Nos. 2 and 3) is shown in Figure 5. The imbibition process for both cores exhibits distinct staged characteristics:

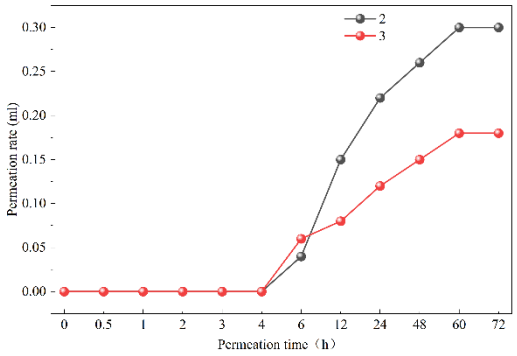


Figure 5. The variation of imbibition volume over time for the two core samples (Nos. 2 and 3)

The results of the 72-hour static imbibition experiment indicate that the imbibition process of the two core samples exhibits distinct staged characteristics. The period of 0–4 h is the start-up lag phase, during which the imbibition volume is zero, representing a transitional stage for water-phase wetting and capillary pressure establishment. The period of 4–60 h is the rapid rise phase, during which the imbibition volume increases significantly with time; Core No. 2 shows a faster increase rate, reaching a final imbibition volume of 0.30 mL, which is significantly higher than that of Core No. 3 (0.18 mL). Although the imbibition volume of Core No. 3 briefly exceeds that of Core No. 2 around 6 h, its later-stage increase is weak, indicating an overall lower imbibition capacity. The period of 60–72 h is the equilibrium stabilization phase, during which the imbibition volume tends to stabilize, and the residual oil becomes difficult to displace further due to capillary trapping. The experiments confirm that Core No. 2 exhibits better spontaneous imbibition oil displacement performance. Differences in pore structure and wettability are the main reasons for the observed differences in imbibition effectiveness, providing experimental support for optimizing imbibition oil recovery in the target reservoir.

5. CONCLUSION

(1)The low-permeability reservoir rocks in the study area exhibit high brittleness and high stiffness. High-pressure water injection can reduce the effective stress and weaken the rock strength, promoting the initiation and propagation of micro-fractures, thereby providing favorable mechanical conditions for fracture creation and permeability enhancement via pressure-driven water injection.

(2)The displacement pressure differential and injection rate synergistically enhance the reservoir seepage capacity, with the improvement in permeability being far greater than that in porosity. When the pressure differential exceeds 10 MPa, the reservoir enters a rapid permeability-enhancement stage, and at 50 MPa, the permeability increases to 7.25 times its initial value. Medium-to-high injection rates can intensify fluid shear action, further widening fracture channels and establishing a pore–fracture composite seepage system.

(3)Increasing the displacement pressure significantly optimizes the oil–water two-phase seepage characteristics, expands the two-phase co-permeability interval, reduces residual oil saturation, enhances water-phase flow capacity, effectively improves waterflood sweep efficiency, and increases the degree of crude oil mobilization.

(4)Spontaneous imbibition in low-permeability cores exhibits a three-stage characteristic of "lag–rise–stabilization." Differences in pore connectivity result in better imbibition performance for Core No. 2 than for Core No. 3. Imbibition can effectively mobilize a portion of the residual oil and serves as an important supplement for tapping remaining oil after pressure-driven water injection.

REFERENCES

[1] Dang, X. X. (2018). Analysis of the development status and prospects of low-permeability oil reservoirs in China. *Petrochemical Technology*, *25*(12), 149.

[2] Zhang, C. F., Qi, Z. Z., Wu, Z. P., et al. (2025). Thermal simulation experiments of kerogen in hydrocarbon source rocks of Bayingogobi Formation in Chaghang Depression. *Block Oil and Gas Field*, *32*(04), 536–542.

[3] Du, Y. F., Li, R. X., Xing, Z. M., et al. (2026). Evaluation of brittleness based on microscopic-macroscopic rock mechanics characteristics and its application in hydraulic fracturing: A case study of the Qionzhusi Formation shale reservoir in southern Sichuan. *China Geology*, *53*(02), 449–465. https://doi.org/10.12029/gc20250716002.

[4] Cheng, Q., Wu, J. T., Liu, W. C., et al. (2026). Evaluation of the brittleness of metamorphic rock reservoirs based on rock mechanical properties and its main control factors: A case study of Bohzhong 19-6 Gas Field. *Geological Bulletin*, *45*(04), 693–707. https://doi.org/10.12097/gbc.2025.10.082.

[5] Li, L., Tian, W., Bai, X. H., et al. (2023). Experimental and understanding of gas-water flow in horizontal well casing under different completion methods. *Drilling and Production Technology*, *46*(04), 71–76.

[6] Gao, H., Wang, Z. M., Wang, X. Z., et al. (2017). Experimental study on variable mass flow flow in a sand-transporting well with oil, gas and water trifuel. *Special Oil and Gas Reservoirs*, *24*(04), 147–151.

[7] Jia, C. Y., Tao, L. Y., Wang, H. M. (2025). Research progress on spontaneous percolation mechanism and recovery rate evaluation during hydraulic fracturing in low-permeability oil reservoirs. *Oil and New Energy Sources*, *37*(05), 77–90.